БИОТЕХНОЛОГИЯ, 2022, том 38, № 3, с. 3–21

ПРОДУЦЕНТЫ, БИОЛОГИЯ, СЕЛЕКЦИЯ, ГЕНЕТИЧЕСКАЯ ИНЖЕНЕРИЯ

УДК 579.6+577.1

MAXIMAL BIOMASS YIELD FROM NAPHTHALENE: A THEORETICAL ESTIMATION BASED ON FEATURES OF CELL METABOLISM

© 2022 г. I. G. Minkevich[1], *, I. A. Kosheleva[1], and A. M. Boronin[1]

[1]G.K. Skryabin Institute of Biochemistry and Physiology of Microorganisms, FRC Pushchino Centre for Biological Research, Russian Academy of Sciences, Pushchino, Moscow Region, 142290 Russia

**e-mail minkevich@ibpm.pushchino.ru*

Received April 24, 2022; Revised May 25, 2022; Accepted June 2, 2022

Metabolic pathways of naphthalene conversion to a set of biomass formation precursors, including the whole patterns of the biochemical reaction rates, were found by computer reconstruction. Stoichiometric coefficients of the reactions and the data on their reversibility or irreversibility were used. The computed rates of the precursor synthesis and application of the metabolism bioenergetic regularities gave maximal biomass yield values. It was found that the presence of *meta*, *ortho* or gentisate-mediated paths of naphthalene oxidation exerted a lesser effect on the yield value than the operation of the TCA cycle via the full sequence or glyoxylate bypass. The latter factor markedly affected the values of flows via gluconeogenesis and the pentose phosphate pathway. The maximal biomass yield from naphthalene was found to be within the range of 0.75–0.86 g/g. The maximal part of naphthalene energy incorporated into grown biomass was found to be nearly 1/3.

Keywords: Naphthalene degradation, bacteria, cell metabolism, stoichiometry of reaction sets, biomass yield, bioenergetics

DOI: 10.56304/S0234275822030061

INTRODUCTION

Naphthalene is one of polycyclic aromatic hydrocarbons (PAHs), which are a class of widespread environmental pollutants. Many PAHs are known to be toxic, mutagenic, carcinogenic compounds persistent in the environment. In response to contamination, indigenous populations of microorganisms exhibit a remarkable ability to degrade such pollutants. When the biodegradative activity of microflora present in contaminated soil is insufficient or absent, bacteria with a degradation capacity can be introduced *in situ* into the soil of the site.

Bacterial species from soil microflora displaying the ability to degrade various PAHs belong to *Proteobacteria* (*Pseudomonas*, *Pseudoxanthomonas*, *Comamonas*, *Burkholderia*, and *Novosphingobium*), *Firmicutes* (*Bacillus* and *Paenibacillus*), and *Actinobacteria* (*Rhodococcus* and *Arthrobacter*). Naphthalene has been used in research laboratories as a model to develop catalysts and a biological process with potential to effectively destroy various PAHs.

The majority of reported naphthalene degradation pathways in bacteria are aerobic and can be subdivided into two stages. Reactions of the upper stage transform naphthalene to salicylate. The lower stage converts salicylate to tricarboxylic acid cycle intermediates. Depending on the organism, the formed salicylate is further metabolized either via the catechol route using salicylate 1-hydroxylase, or the gentisate route employing salicylate 5-hydroxylase. Further, catechol is ring-cleaved through the *meta* route by catechol 2,3-dioxygenase or alternatively through *ortho*-pathway using catechol 1,2-oxygenase . In the gentisate pathway, the aromatic ring is cleaved by gentisate 1,2-dioxygenase to produce maleylpyruvate. Gram-negative microorganisms such as *Pseudomonas* perform salicylate decarboxylation by salicylate 1-hydroxylase to form catechol. In Gram-positive bacteria (*Rhodococcus*), salicylate is converted to gentisate usually by salicylate 5-hydroxylase.

Estimation of PAH biodegradation efficiency is necessary for comparison and selection of the most promising microbial strains for environmental protection. This efficiency depends on some parameters, the most significant of which are the rate of the biodegradation process and the yield of biomass during its growth on a target substrate, as well as the size of the degrader inoculum applied to the contaminated soil. The rate of biomass growth and the yield of biomass from the substrate are important from the viewpoint of both the inoculum production and the contaminant degradation in soil. These parameters are also of interest from the viewpoint of the physiology and bioenergetics of microbial population growth on a given substrate.

List of abbreviations: PAHs – polycyclic aromatic hydrocarbons, SCM – standard constructive metabolism, FM – full forward metabolism, GenMetPath – Generator of Metabolic Pathways.

Most publications on naphthalene biodegradation are devoted to experimental research into the completeness of naphthalene consumption by a strain or into the metabolic pathways of naphthalene oxidation by various bacteria as well as genes responsible for the presence of such paths in cells. The pathways, as a rule, are considered from the stage of the degraded pollutant primary oxidation to formation of one of the known metabolites involved in "usual" cell metabolism such as, e.g., pyruvate, acetaldehyde, succinyl-CoA [1–7]. Details of the further conversion of these products and the functioning of the whole metabolism remain obscure. Experimental data on the biomass yield from naphthalene available in the literature are scarce [8, 9] because of a considerable complexity of such measurements.

For this reason, the theoretical estimation of the attainable yield value based on the data about naphthalene metabolism in cells is of great interest. Such an estimate makes it possible to find how close the experimentally obtained yield values are to the possible maximum and, correspondingly, to what extent the applied growth conditions are close to the optimum.

This estimation is, in fact, an investigation of the metabolism's influence on the characteristics of cell population growth. Therefore, it requires revealing a pattern of metabolic flows responsible for transformation of substrate into cell biomass including those supplying energy for the process. Finding this pattern is both an intermediary tool for the yield value calculation and an independent result of its own significance for knowledge of living cell physiology.

Theoretically, the stoichiometry of the whole metabolism might be ascertained if all the involved reactions and flows via them had been known. In reality, full information of this kind is not available. Therefore, the stated problem was solved by accepting the growth on the best studied substrate as a reference process and finding metabolic differences between this process and growth on the substrate of interest.

To accomplish this task, the whole cell metabolism was subdivided into standard constructive metabolism (SCM) and full forward metabolism (FM) [10]. The former consists of practically identical pathways during the growth of various organisms on any substrate. SCM contains the most part of reactions forming the whole metabolism. On the contrary, FM contains essentially a smaller number of reactions and strongly depends on a growth substrate.

The input substances of SCM are, first of all, the precursors of biomass synthesis which have been called as nodal metabolites [10, 11]. They are: glucose as a precursor of cellular carbohydrates; acetyl-CoA from which cells synthesize lipids; 2-oxoglutarate, erythrose-4-phosphate, oxaloacetate, ribose-5-phosphate, 3-phosphoglycerate, phosphoenolpyruvate, and pyruvate as precursors of protein and nucleic acid formation. Further, SCM requires NADPH as a source of additional reductivity for adjustment of the whole nodal metabolite reductivity to that of cell biomass and ATP as a source of high-energy bonds for synthesis of biomass constituents. We take into account that the exchanges NADH $\rightleftharpoons$ NADPH and ATP $\rightleftarrows$ GTP proceed in cells easily.

As a reference substrate, glucose has been chosen since the growth on it as well as its metabolism were the best studied. Various microorganisms grown on glucose at optimal conditions showed the same yield equal to 0.5. The method for calculation of SCM characteristics based on the data concerning glucose metabolism was developed in our work [10]. It is described in brief below (**MATERIALS AND METHODS** section).

The nodal metabolites as well as NADPH and ATP are formed in FM by conversion of an organic substrate, the yield from which is the quantity of interest. Other substrates of FM are ADP, $NADP^+$, CoA, H_3PO_4, and, in the case of aerobic growth, oxygen. These compounds, except oxygen, are cyclically returned to FM by SCM after consuming ATP, NADPH and various AcylCoA.All reactions constituting the FM on a given substrate (naphthalene in our case) and flows via them can be found using a specially designed computer program package GenMetPath (Generator of Metabolic Pathways). The mathematical basics of this program are described in detail elsewhere [11–13] and briefly in **MATERIALS AND METHODS** below.The biomass yield from a substrate, which is a source of substance and energy for growth, depends on the specific growth rate as follows [14, 15]:

$$Y_{X/S} = \frac{Y_{X/S}^{max}\mu}{m_S Y_{X/S}^{max} + \mu}, \quad (1)$$

where $Y_{X/S}$ is dry cell biomass yield, g/g; μ is specific growth rate, h^{-1}; $Y_{X/S}^{max}$ is maximum biomass yield, and m_S is the specific rate of the substrate expenditure for cell maintenance, h^{-1}.

The quantities $Y_{X/S}^{max}$ and m_S are physiological and bioenergetic parameters of the strain. They depend on the growth conditions, e.g., temperature and pH. According to Eq. (1), $Y_{X/S} = 0$ at $\mu = 0$ and asymptotically approaches the value $Y_{X/S} = Y_{X/S}^{max}$ during μ increase. At a growth rate μ notably higher than m_S the values of $Y_{X/S}$ become close to $Y_{X/S}^{max}$. At μ nearly equal to $m_S Y_{X/S}^{max}$ the biomass yield is approximately twice as low as its maximal value $Y_{X/S}^{max}$.

The value of m_S depends on the rate of matter turnover in cells. At present the problem of the theoretical calculation of this quantity seems hardly solvable and its values should be determined experimentally. The order of m_S for a given strain can be found based on the

data related to other microorganisms cultivated at optimal growth conditions. At the same time, the value of $Y_{X/S}^{max}$ attainable for a given strain grown on a given substrate at optimal conditions can be calculated using the method mentioned above.

The mass yield $Y_{X/S}$, which is commonly used as a stoichiometric index of substrate conversion to biomass, does not reflect the energetic efficiency of such conversion. The latter is estimated by energetic growth yield $\eta_{X/S}$ which represents a fraction of substrate energy incorporated into the biomass grown. The latter quantity depends on specific growth rate in a form similar to that of the mass yield [15]:

$$\eta_{X/S} = \frac{\eta_{X/S}^{max}\mu}{m_e\eta_{X/S}^{max} + \mu}, \qquad (2)$$

where m_e is the specific rate of substrate energy expenditures for cell maintenance, $\eta_{X/S}^{max}$ is maximal cell energetic yield attainable when cell maintenance processes play a minor role in the metabolism.

The quantities $\eta_{X/S}$, $\eta_{X/S}^{max}$, and m_e are expressed in units of organic matter reductivity [15–20] as described in **MATERIALS AND METHODS**.

The present work solves the following tasks: 1) finding metabolic flows via the forward metabolism FM of microorganisms growing on glucose and, on this basis, calculating the nodal metabolite, NADPH and ATP inflows of standard constructive metabolism; 2) finding metabolic flows via FM of bacteria utilizing naphthalene as the sole source of organic matter and energy, and 3) using these results, calculating maximal cell yield values, by mass and by energy for naphthalene degrading bacteria. The corresponding techniques are described in **MATERIALS AND METHODS**.

MATERIALS AND METHODS

Theoretical background of the computer program package GenMetPath

The GenMetPath program package was developed by I.G. Minkevich for finding reactions which make up a required metabolic pathway. The reactions are selected from a local database (placed in the researcher's computer). The approach underlying the calculations uses stoichiometric equations which are linear algebraic [12, 15, 21]. The stoichiometric coefficients of all reactions from the local database form a matrix ν_{kr} where k is the number of a compound in the total set of reagents participating in all reactions present in the local database; r is the number of a reaction. The r'th column of ν_{kr} describes the stoichiometry of the r'th reaction. Zero elements of this column relate to substances not participating in the given reaction. Elements of k'th row of ν_{kr} participate in the molar balance of the k'th compound during the operation of all reactions. A system of reactions gets several substances as outer substrates and passes some of the formed compounds outside as system products. The rates of exchange between the reaction system and its surroundings form a vector b_k.

The equation system describing the stoichiometry of the whole reaction system is as follows:

$$\sum_r \nu_{kr} z_r = b_k \text{ for all values of index } k, \qquad (3)$$

where each z_r is the molar flow via the r'th reaction. When the values of b_k are assigned and z_r are unknown the latter quantities should be found by solving Eqs. (3).

Direct application of standard algorithms for solution of linear algebraic equations meets difficulties specific to this problem [11–13]. Firstly, a part of b_k components cannot be assigned initially. When finding the reactions composing a forward metabolism, the synthesis rates of nodal metabolites, ATP, NADPH should be set. But the rates of an organic substrate and oxygen consumption, and CO_2, H_2O formation cannot be known beforehand and should be calculated. Equations for numbers k corresponding to the latter components are to be excluded from Eqs. (3) and used for these b_k calculation after all z_r are found.

Secondly, the number of unknown z_r's is, as a rule, higher than the number of equations, especially after the mentioned reduction of the system Eqs. (3). Therefore, the values of a part of z_r's should be initially set after which the remaining z_r's can be found from thus transformed Eqs. (3). The existence of several variants of this z_r's setting results in the existence of several variants of metabolic pathways converting the growth substrate into the nodal metabolites. In cells these variants can be realized both singly and as a linear combination of at least two variants. In the latter case the interrelation between flows in the branching points of metabolism depends on kinetic regulation of the corresponding enzyme rates. An example of such branching is flow partition between full tricarboxylic acid cycle and its truncated variant via glyoxylate bypass.

Finally, some reactions are irreversible which imposes constraints upon the corresponding z_r such as $z_r \geq 0$. This fact introduces restrictions upon the region of z_r values within which the solution is situated. The details of mathematical formulation and solution of the latter problem are described by Minkevich [11–13].

The local database used in this work contains the stoichiometry of biochemical reactions and information about their reversibility or irreversibility. It includes 115 reactions and 112 compounds. The names of the reactions and compounds (the full list of substrates and products of the reactions) are given in Tables A1 and A2 in **Appendix**. The reactions relate, first

of all, to the metabolic pathways usually present in living cells: glycolysis and gluconeogenesis, pentose phosphate pathway, tricarboxylic acid cycle with glyoxylate bypass, a number of reactions of the central metabolism. Further, this database includes reactions of metabolization of naphthalene and other aromatics, and C1 compounds. For other problems the database can be easily expanded.

It should be emphasized that two malate dehydrogenases, NAD-dependent and quinone-dependent, present in the local database, catalyze irreversible reactions. The NAD-dependent reaction forms malate from oxaloacetate which is a process inverse to TCA direction. But the quinone-dependent reaction proceeds from malate to oxaloacetate and, therefore, is a proper constituent of the TCA cycle. There are a number of works which have found evidence of the presence of the latter enzyme in bacteria [22–27].

Energetic characteristics of cell metabolism

These characteristics are closely associated with reductivity as a parameter of various substances participating in the metabolism. In this work the notion of reductivity has been applied for balance analysis of the standard constructive metabolism and for calculation of the total energy efficiency of bacterial growth on naphthalene during the operation of different pathways of this substrate consumption.

The general unit of reductivity is redoxon (RO) introduced by Minkevich [19]. The number of RO's is a measure of how much a given compound is reduced relative to a common zero reductivity level. The latter is assigned to carbon dioxide, water, ammonia, orthophosphate, proton, etc., in the standard biochemical state (t° = 25°C, pH 7.0). These compounds were called as basis substances. The precursor of RO is the notion of available electrons [16, 17, 28]. Reductivity measured in RO's, and earlier in available electrons, was applied for solution of a number of problems related to the mass-energy balance of cell metabolism and cultivation of microorganisms [15–18, 20, 29, 30] and displayed itself as a powerful tool in this field.

The definition of RO is based on the equation of any compound formation by reduction of the proper number of basis substances:

$$\begin{aligned} &HCO_3^- + H_2O + H^+ + NH_4^+ + H_2PO_4^+ \\ &\quad + H_2S + Fe^{3+}\ldots + \left[-\left(1/4\right)O_2\right] \rightarrow \\ &\rightarrow C_{a_C}H_{a_H}O_{a_O}N_{a_N}P_{a_P}S_{a_S}Fe_{a_{Fe}}\ldots^{(E)}, \end{aligned} \qquad (4)$$

where $C_{a_C}H_{a_H}O_{a_O}N_{a_N}P_{a_P}S_{a_S}Fe_{a_{Fe}}\ldots^{(E)}$ is the molar formula of the formed compound, a_C, a_H, etc. are atomic numbers of chemical elements in the formed molecule, E is its electric charge, and $\left[-\left(1/4\right)O_2\right]$ is an amount of oxygen subtracted from the basis substances in order to reduce them to the level of the formed compound. RO corresponds to one $\left[-\left(1/4\right)O_2\right]$ unit, i.e., to one place for an electron which can be accepted by free oxygen during a reverse process of the compound oxidation to basis substances.

Balancing of Eq. (4) by all chemical elements gives the following number of RO's per 1 mole of the compound considered: $\alpha = 4a_C + a_H - 2a_O - 3a_N + \ldots - E$ where α is the molar reductivity of the compound (the number of RO's per its 1 mole). A useful quantity is the average reductance degree of carbon, $\gamma = \alpha/a_C$, which is applicable to both individual organic compounds and their mixture including dry cell biomass. In the latter case it is suitable to use the gross elemental composition of dry biomass expressed per 1 carbon atom: $CH_{b_H}O_{b_O}N_{b_N}\ldots$ Then $\gamma = 4 + b_H - 2b_O - 3b_N + \ldots$.

Organic substances have positive α and γ values. Oxygen is a particular substance due to its role in the formation of a compound; therefore, it has the negative number of RO's: –4 per one O_2 molecule. All reactions proceed under the laws of conservation of each chemical element and the electric charge from which there follows the law of RO conservation: the total number of RO's of reaction substrates equals the total number of RO's of reaction products.

The energetic properties of redoxon are described below.

The rates of biochemical reactions, both individual and their aggregates (in other words, metabolic flows), can be easily recalculated to RO units. Denoting the molar flow as F^{mol} and its expression in RO's as f, we have: $f = \alpha F^{mol}$. Denoting the flows in grams as F^{mass}, we obtain for carbonaceous substances: $f = \frac{\sigma\gamma}{12}F^{mass}$, where σ is the mass fraction of carbon in the substance to which the flow F^{mass} relates, $\frac{\sigma}{12}F^{mass}$ is the corresponding flow in moles of the substance carbon.

Let subscripts S and B relate to the substrate and biomass, correspondingly. Then, taking a ratio of expression $f_B = \frac{\sigma_B\gamma_B}{12}F_B^{mass}$ for cell biomass to that for the growth substrate, $f_S = \frac{\sigma_S\gamma_S}{12}F_S^{mass}$, we obtain: $\frac{f_B}{f_S} = \frac{\sigma_B\gamma_B}{\sigma_S\gamma_S}\frac{F_B^{mass}}{F_S^{mass}}$. The ratio $\frac{F_B^{mass}}{F_S^{mass}} = Y_{X/S}$ is the mass yield of dry cell matter from the substrate. We introduced the biomass yield from the substrate by RO's (formerly the yield by available electrons), $\eta_{X/S}$, as follows:

$$\frac{f_B}{f_S} = \eta_{X/S} \qquad (5)$$

[15–20]. Then, the interrelation between both expressions of biomass yield is as follows:

$$\eta_{X/S} = \frac{\sigma_B\gamma_B}{\sigma_S\gamma_S} Y_{X/S}, \quad Y_{X/S} = \frac{\sigma_S\gamma_S}{\sigma_B\gamma_B}\eta_{X/S}. \qquad (6)$$

The values of σ_S and γ_S can be easily calculated from the substrate elemental composition. For various nonoleaginous microorganisms it was found from our and literature data on dry biomass elemental composition that $\sigma_B\gamma_B$ is close to 1.9 [15].

An important property of organic substances, both individual compounds and dry cell biomass, is that their energy level expressed per one RO is close to the same value: 113–114 kJ (nearly 27 kcal) per RO mole [15, 16, 19]. Therefore, $\eta_{X/S}$ is close to a fraction of the substrate energy store which is incorporated into the biomass grown. This quantity is independent of substrate energy content per one mole or one gram of the substance. Therefore, $\eta_{X/S}$ is the most correct criterion for the comparison of growth efficiency on different substrates. The value of $\eta_{X/S}$ is always lower than 1. The highest $\eta_{X/S}$ was achieved during the growth of various microorganisms on glucose: $\eta_{X/S} = 0.6$ [10, 15].

The balance of reductivity for metabolic flows has a very simple form. In the case of aerobic growth when organic products are absent or inconsiderable this balance is as follows:

$$f_S = f_B + f_{O_2}, \qquad (7)$$

where f_{O_2} is the total flow of RO's via all paths where O_2 is a terminal acceptor of electrons. Since the O_2 molecule accepts 4 electrons,

$$f_{O_2} = 4F^{mol}_{O_2}. \qquad (8)$$

Values of flows on the input of standard constructive metabolism

The approach for calculation of these flows is described in detail elsewhere [10]. It is based on the following regularities. i) The metabolism of cells growing on glucose was assumed as a reference one. Since glucose-consuming cells grow at optimal conditions with a high specific growth rate μ, the highest values of mass yield $Y_{X/S}$ achieved during the cultivation process, according to Eq. (1), are very close to $Y^{max}_{X/S}$. Therefore, $Y^{max}_{X/Glucose} = 0.5$ and $\eta^{max}_{X/Glucose} = 0.6$ were taken as the reference biomass yield values. ii) It was found earlier that σ and γ for both lipid-free and lipidic fractions of dry cell biomass are considerably constant [29]. For lipid-free biomass the values of these quantities are very close to those for glucose: $\sigma_{B0} = 0.4$ and $\gamma_{B0} = 4$.

The balances of RO's and carbon during the conversion of nodal metabolites to biomass have been considered from which the additional amount of reductivity in the form of NADPH which should be supplied to SCM was found. The latter is necessary for adjusting the average carbon fraction and reductivity in the total flow of nodal metabolites to the mentioned σ_{B0} and γ_{B0} values. A similar approach was applied for calculation of NADPH necessary for synthesis of the lipid biomass fraction from glucose via Acetyl-CoA. In this way the flow f_B was found. Further, the amount of oxygen consumed during the growth on glucose was calculated using $\eta_{X/S} = 0.6$. Equation (7) gives: $\frac{f_{O_2}}{f_B} = \frac{f_S}{f_B} - 1 = \frac{1}{\eta_{X/S}} - 1 = \frac{2}{3}$, from which and from Eq. (8): $F^{mol}_{O_2} = \frac{1}{4} f_{O_2} = \frac{1}{6} f_B$. Thereby the flows of all nodal metabolites and NADPH on the input of SCM and, correspondingly, the output of FM as well as the rate of O_2 on the FM input *on glucose* were found including the amount of ATP which is necessary (including ATP converted to GTP) for energy requirements of SCM.

Table 1. Nodal metabolites and the rates of their formation by forward metabolism

Nodal metabolites	Flows, mmol/h
Acetyl-CoA	18.9
D-Glucose	2
3-Phosphoglycerate	4.8
Phosphoenolpyruvate	4.8
Pyruvate	4.8
2-Oxoglutarate	3
Oxaloacetate	4.8
D-Ribose 5-phosphate	2.4
D-Erythrose 4-phosphate	3
ATP	382
NADPH	34.8

The rates of all compounds on the input of SCM obtained as described here are given in Table 1. They correspond to the biomass-growth volumetric rate of 3.82 g/h and can be proportionally recalculated for another growth rate value.

Calculation of biomass yield from naphthalene

The maximal yields of dry cells from naphthalene by mass, $Y^{max}_{X/S}$, and by RO's, $\eta^{max}_{X/S}$, were calculated as follows. Application of GenMetPath program to FM on naphthalene with established output flow values given in Table 1 and unknown values of F^{mol}_S and $F^{mol}_{O_2}$ resulted in finding the latter flows. They provide the matter and energy requirements of only SCM and do not provide the requirements of cell maintenance. Therefore, the biomass yield calculated from F^{mol}_S and

$F_{O_2}^{mol}$ is $Y_{X/S}^{max}$ in mass units and $\eta_{X/S}^{max}$ in RO units (see Eqs. (1) and (2)).

Recalculation of F_S^{mol} to RO units was made using the interrelation $f_S = \alpha_S F_S^{mol}$. The elemental composition of naphthalene is $C_{10}H_8$ from which $\alpha_S = 4a_C + a_H = 48$, $\sigma_S = 12a_C/(12a_C + a_H) = 15/16$, $\gamma_S = \alpha_S/a_C = 4.8$, $\sigma_S\gamma_S = 4.5$. As mentioned above, $\sigma_B\gamma_B = 1.9$. Then, application of Eqs. (5)–(7) gives:

$$\eta_{X/S} = (f_S - f_{O_2})/f_S = \left(48F_S^{mol} - 4F_{O_2}^{mol}\right)/48F_S^{mol}, \quad (9)$$
$$Y_{X/S} = 2.368\eta_{X/S}.$$

Comparison of biomass yield values from naphthalene and n-alkanes

Let us compare the microbial growth on two different substrates with identical $\eta_{X/S}$ values. Then, writing the right expression (6) for substrates 1 and 2 and taking their ratio, we obtain: $\frac{Y_{X/S2}}{Y_{X/S1}} = \frac{\sigma_{S2}\gamma_{S2}}{\sigma_{S1}\gamma_{S1}}$. Let substrate 1 be long-chain *n*-alkanes with a gross formula CH_2, from which $\sigma_{S1} = \frac{12}{14}$, $\gamma_{S1} = 6$, $\sigma_{S1}\gamma_{S1} = \frac{36}{7} \approx 5.143$. For naphthalene as substrate 2 we obtained above $\sigma_S\gamma_S = 4.5$. Then,

$$\frac{Y_{X/\text{naphthalene}}}{Y_{X/n\text{-alkanes}}} = \frac{\sigma_{S2}\gamma_{S2}}{\sigma_{S1}\gamma_{S1}} = \frac{4.5}{5.143} = 0.875. \quad (10)$$

Values of cell yield from naphthalene by full mass and by carbon

Sometimes the cell yield is expressed as the ratio of grown biomass carbon to the substrate consumed carbon (denoted as $y_{X/S}$). Then the full mass yield, $Y_{X/S}$ relates to $y_{X/S}$ as

$$Y_{X/S} = \frac{\sigma_S}{\sigma_B} y_{X/B}. \quad (11)$$

RESULTS AND DISCUSSION

The values of the rates at which SCM consumes nodal metabolites, NADPH and ATP, are given in Table 1. They correspond to the biomass-growth volumetric rate of 3.82 g/h and can be proportionally recalculated for another growth rate value (see **MATERIALS AND METHODS**). The same relates to all rates of biochemical reactions given below.

The full set of flows via the reactions composing the forward metabolism, which transforms naphthalene to nodal metabolites, was determined separately for the above mentioned three pathways. For every pathway these sets were found for two variants of tricarboxylic acid (TCA) cycle operation. It can function in its complete form (citrate → isocitrate → succinyl-CoA → succinate → fumarate → malate → oxaloacetate) or in a truncated form via the glyoxylate bypass. The latter variant operates, e.g., during microbial growth on n-alkanes. The results are shown in Tables 2–4. The values of some rates given in these tables are equal to zero or are small compared with those in Table 1, which means that the corresponding enzymes do not participate in the forward metabolism or their role in it is negligible.

One of the *meta* pathway variants (except the electron transport chain) is present in Fig. 3. The full stoichiometric equation describing this case of naphthalene conversion to the nodal metabolites shown in Fig. 3 is as follows:

$267.5O_2 + 397H_3PO_4 + 382ADP + 34.8NADP^+ +$
$+ 18.9CoA + 34.9Naphthalene = 197.7CO_2 +$
$+ 394.7H_2O + 34.8H^+ + 382ATP + 34.8NADPH +$
$+ 18.9Acetyl\text{-}CoA + 2D\text{-}Glucose + 4.8 \times 3\text{-}Phosphoglycerate + 4.8Phosphoenolpyruvate + 4.8Pyruvate +$
$+ 3 \times 2\text{-}Oxoglutarate + 4.8Oxaloacetate + 2.4D\text{-}Ribose\ 5\text{-}phosphate + 3D\text{-}Erythrose\ 4\text{-}phosphate.$

Figures 1 and 2 depict the FM (also except the electron transport chain) for *ortho* and gentisate-mediated pathways of naphthalene oxidation, correspondingly. The full stoichiometric equation of FM for the *ortho* path is as follows:

$289.2O_2 + 397H_3PO_4 + 382ADP + 34.8NADP^+ +$
$+ 18.9CoA + 36.7Naphthalene = 215.8CO_2 + 401.9H_2O +$
$+ 34.8H^+ + 382ATP + 34.8NADPH + 18.9Acetyl\text{-}CoA +$
$+ 2D\text{-}Glucose + 4.8 \times 3\text{-}Phosphoglycerate +$
$+ 4.8Phosphoenolpyruvate + 4.8Pyruvate + 3 \times 2\text{-}Oxoglutarate + 4.8Oxaloacetate + 2.4D\text{-}ribose\ 5\text{-}phosphate + 3D\text{-}erythrose\ 4\text{-}phosphate.$

The same for the gentisate-mediated path:

$266.7O_2 + 397H_3PO_4 + 382ADP + 34.8NADP^+ +$
$+ 18.9CoA + 34.8Naphthalene = 197CO_2 + 394.4H_2O +$
$+ 34.6H^+ + 382ATP + 34.8NADPH + 18.9Acetyl\text{-}CoA +$
$+ 2D\text{-}glucose + 4.8 \times 3\text{-}Phosphoglycerate +$
$+ 4.8Phosphoenolpyruvate + 4.8 \times Pyruvate + 3 \times 2\text{-}Oxoglutarate + 4.8Oxaloacetate + 2.4D\text{-}ribose\_5\text{-}phosphate + 3D\text{-}Erythrose\_4\text{-}phosphate.$

Table 5 gives the summary set of the maximal $Y_{X/S}^{max}$ and $\eta_{X/S}^{max}$ values obtained for all variants of the biochemical pathways considered above.

For all the three variants of naphthalene metabolization (the *ortho*, *meta* pathways and the pathway via gentisate) the molar flows from primary naphthalene oxidation up to metabolites common for "usual" cell metabolism have uniform values. The first reaction with a different flow value is that catalyzed by pyruvate carboxylase. The *meta* path includes an alternative sequence of reactions between 2-hydroxymuconate semialdehyde and 2-hydroxy-2,4-pentadienoate. This

Table 2. Forward metabolism (FM) reaction rates, overall input-output FM flow rates and corresponding biomass yield maximal values computed. The case of naphthalene oxidation via the *ortho* pathway. Variant 1: full tricarboxylic acid cycle; variant 2: glyoxylate bypass

Reactions	1	2
	Flows, mmol h^{-1}	
Naphthalene 1,2-dioxygenase	36.7	39.6
cis-1,2-Dihydro-1,2-dihydroxynaphthalene dehydrogenase	36.7	39.6
1,2-Dihydroxynaphthalene dioxygenase	36.7	39.6
2-Hydroxychromene-2-carboxylate isomerase	36.7	39.6
trans-o-Hydroxybenzylidenepyruvate hydratase-aldolase	36.7	39.6
Salicylaldehyde dehydrogenase	36.7	39.6
Salicylate 1-monooxygenase	36.7	39.6
Catechol 1,2-dioxygenase	36.7	39.6
Muconate cycloisomerase	36.7	39.6
Muconolactone delta-isomerase	36.7	39.6
3-Oxoadipate enol-lactonase	36.7	39.6
3-Oxoadipate CoA-transferase	36.7	39.6
3-Oxoadipyl-CoA thiolase	36.7	39.6
Pyruvate carboxylase	9.6	32.4
Pyruvate dehydrogenase complex	22.3	2.45
Citrate synthase	40.1	13.1
Aconitase	40.1	13.1
Isocitrate dehydrogenase	40.1	3
Oxoglutarate dehydrogenase	37.1	0
Succinyl coenzyme A synthetase (GTP)	37.1	0
Succinate dehydrogenase (complex II)	73.8	49.7
Fumarase (fumarate hydratase)	73.8	49.7
Quinone-dependent malate dehydrogenase	73.8	59.8
Isocitrate lyase	0	10.1
Malate synthase	0	10.1
Phosphoenolpyruvate carboxykinase (ATP)	38.5	74.25
Enolase	33.7	69.45
Phosphoglycerate mutase	33.7	69.45
Phosphoglycerate kinase	28.9	64.65
Glyceraldehyde phosphate dehydrogenase (phosphorylating)	28.9	64.65
Triosephosphate isomerase	21.5	57.25
Fructose bisphosphate aldolase	21.5	57.25
Fructose 1,6-bisphosphatase	21.5	57.25
Glucose-6-phosphate isomerase	52.7	160
Glucose 6-phosphatase	2	2
Glucose-6-phosphate dehydrogenase	50.7	158
6-Phosphogluconolactonase	50.7	158
Phosphogluconate dehydrogenase (decarboxylating)	50.7	158
Ribose-5-phosphate isomerase	19.5	55.25
D-Ribulose-5-phosphate 3-epimerase	31.2	102.7
Transketolase (KEGG R01641)	17.1	52.9
Transaldolase (KEGG R08575)	17.1	52.9
Transketolase (KEGG R01067)	14.1	49.9
$NAD(P)^+$transhydrogenase (AB-specific)	66.6	281
ATP GDP phosphotransferase	37.1	0
ETC (complex I)	137.2	222
ETC (complex III)	284.8	331.4
ETC (complex IV)	142.4	165.7
ATP synthase	422	553.3

Table 2. (Contd.)

Reactions	1	2
Input-output flows, mmol h^{-1}		
Naphthalene consumed	36.7	39.6
O_2 consumed	289	324
CO_2 formed	216	245
H_2O formed	402	413.6
$\eta_{X/S}^{max}$	0.34	0.32
$Y_{X/S}^{max}$, g/g	0.81	0.75

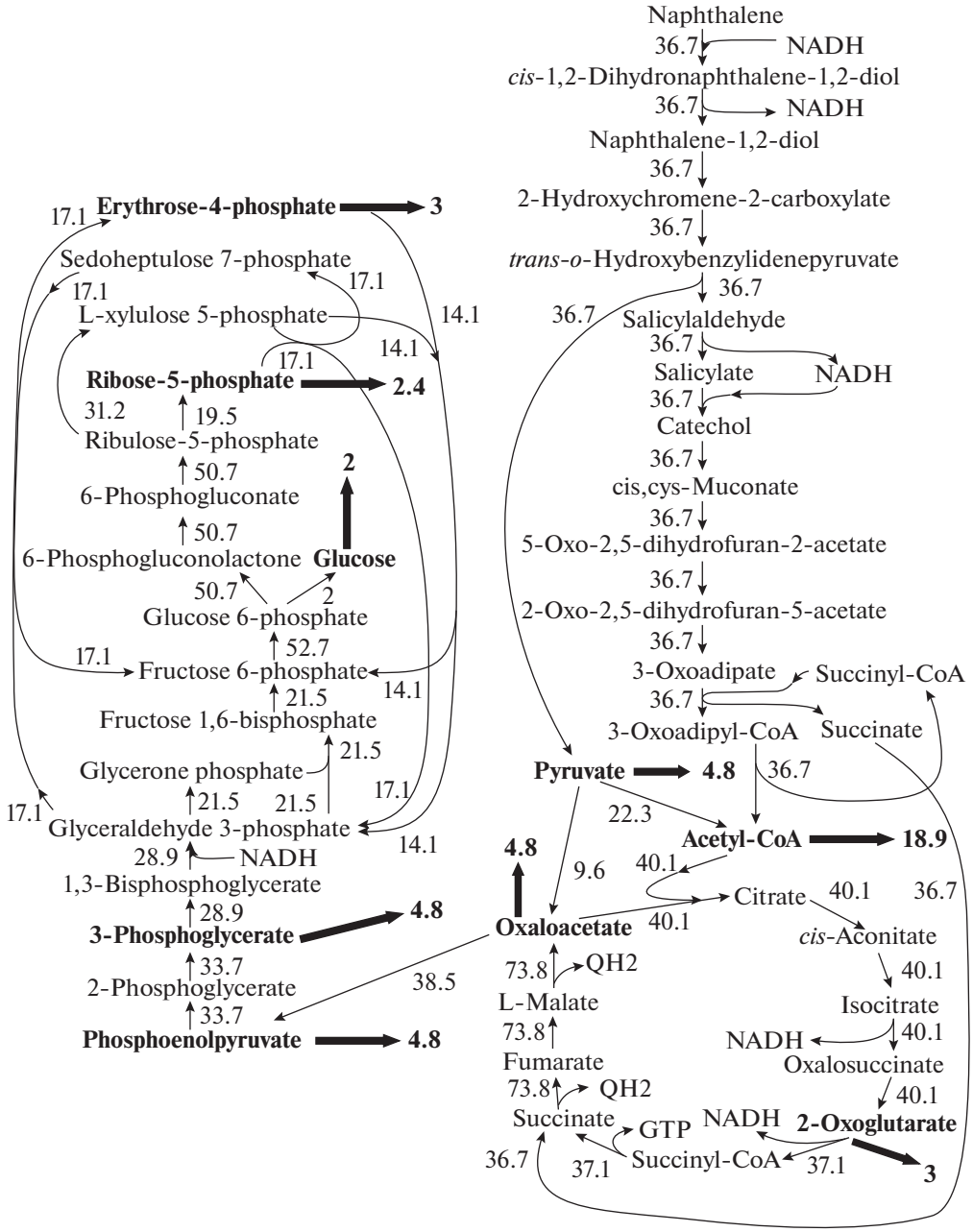

Fig. 1. Scheme of nodal metabolite (NM) synthesis from naphthalene via the *ortho* pathway (variant 1 in Table 2 for $Y_{X/Naphthalene}^{max} = 0.81$). NM names are given by Arial bold. Thick arrows show outflows of NM formed in the forward metabolism to the standard constructive metabolism (see Table 1).

Table 3. Forward metabolism (FM) reaction rates, overall input-output FM flow rates and corresponding biomass yield maximal values computed. The case of naphthalene oxidation via the gentisate pathway. Variant 1: full tricarboxylic acid cycle; variant 2: glyoxylate bypass.

Reactions	1	2
	Flows, mmol h^{-1}	
Naphthalene 1,2-dioxygenase	34.8	37.54
cis-1,2-Dihydro-1,2-dihydroxynaphthalene dehydrogenase	34.8	37.54
1,2-Dihydroxynaphthalene dioxygenase	34.8	37.54
2-Hydroxychromene-2-carboxylate isomerase	34.8	37.54
trans-o-Hydroxybenzylidenepyruvate hydratase-aldolase	34.8	37.54
Salicylaldehyde dehydrogenase	34.8	37.54
Salicylate 5-hydroxylase	34.8	37.54
Gentisate 1,2-dioxygenase	34.8	37.54
Maleylpyruvate isomerase	34.8	37.54
3-Fumarylpyruvate hydrolase	34.8	37.54
Pyruvate carboxylase	2.7	12.3
Pyruvate dehydrogenase complex	62.2	58
Citrate synthase	43.3	21
Aconitase	43.3	21
Isocitrate dehydrogenase	43.3	3
Oxoglutarate dehydrogenase	40.3	0
Succinyl coenzyme A synthetase (GTP)	40.3	0
Succinate dehydrogenase (complex II)	40.3	18
Fumarase (fumarate hydratase)	75.1	55.6
Quinone-dependent malate dehydrogenase	75.1	73.6
Isocitrate lyase	0	18
Malate synthase	0	18
Phosphoenolpyruvate carboxykinase (ATP)	29.7	60
Enolase	24.9	55.3
Phosphoglycerate mutase	24.9	55.3
Phosphoglycerate kinase	20.1	50.5
Glyceraldehyde phosphate dehydrogenase (phosphorylating)	20.1	50.5
Triosephosphate isomerase	12.7	43
Fructose bisphosphate aldolase	12.7	43
Fructose 1,6-bisphosphatase	12.7	43
Glucose-6-phosphate isomerase	26.3	117.5
Glucose 6-phosphatase	2	2
Glucose-6-phosphate dehydrogenase	24.3	115.5
6-Phosphogluconolactonase	24.3	115.5
Phosphogluconate dehydrogenase (decarboxylating)	24.3	115.5
Ribose-5-phosphate isomerase	10.7	41
D-Ribulose-5-phosphate 3-epimerase	13.6	74.4
Transketolase (KEGG R01641)	8.3	38.7
Transaldolase (KEGG R08575)	8.3	38.7
Transketolase (KEGG R01067)	5.3	35.7
NAD(P)+transhydrogenase (AB-specific)	13.8	196.2
ATP GDP phosphotransferase	40.3	0
ETC (complex I)	140	207
ETC (complex III)	255	300
ETC (complex IV)	127.4	149

Table 3. (Contd.)

Reactions	1	2
	Flows, mmol h^{-1}	
ATP synthase	394	505
Input-output flows, mmol h^{-1}		
Naphthalene consumed	34.8	37.5
O_2 consumed	267	300
CO_2 formed	200	224
H_2O formed	394	405
$\eta_{X/S}^{max}$	0.36	0.33
$Y_{X/S}^{max}$, g/g	0.86	0.79

sequence begins from one of the enzymes: 2-hydroxymuconate semialdehyde hydrolase or 2-hydroxymuconate semialdehyde dehydrogenase (see Table 4). Realization of one or another subpath or any combination of them depends on the expression of the corresponding enzyme genes.

Biochemical reactions specific for naphthalene degradation transform this compound into metabolites which can be considered as "usual" or "common" since the reactions of their further conversion are present in all organisms. Usually, these reactions are outside the scope of research into aromatic compound degradation since they are well known. However, the set of these reaction *rates* is not known in advance but represents an important factor affecting the biomass yield. First of all, it is related to the functioning of the tricarboxylic acid cycle.

The rate of TCA cycle operation can be characterized by the flow via citrate synthase. Comparing all the considered cases, it can be seen from Tables 2–4 that this flow changes nearly fourfold, from 13.1 (Table 2) to 45.7 (Table 4). For all the three paths of naphthalene metabolization the rate of citrate synthase operation is higher when TCA works as the full reaction sequence than in the case of glyoxylate bypass. This difference is the largest for the *ortho* pathway (40.1/13.1, i.e., threefold), is less for the gentisate path (43.3/21, i.e., twofold), and the smallest for the *meta* path (45.7/30.2 and 42.5/28.6, i.e., one and a half times). The absence of a part of TCA cycle reactions in the case of the glyoxylate bypass results in a markedly lesser amount of reductivity, which this cycle supplies to the electron transport chain. By the same reason, the amounts of malate and oxaloacetate formed are markedly higher compared with the full TCA cycle operation. This fact, in turn, results in a much higher flow via gluconeogenesis and, then, the pentose phosphate pathway (PPP) reactions in the case of the glyoxylate bypass compared with the full TCA cycle. Dehydrogenases of PPP complete the lack of reduced pyridine nucleotides taking place because of truncated TCA cycle functioning.

It can be seen from the tables that the rate of ATP synthase is higher than the total rate of ATP production by FM (382 mmol/h) necessary for biomass synthesis by SCM: a part of ATP formed is utilized by FM itself, e.g., within gluconeogenesis. The results of Tables 2–4 show also that the ATP synthase works at a markedly (about 5/4 times) higher rate in the case of the glyoxylate bypass. In part, it occurs due to the absence of GTP formation by substrate phosphorylation which is performed by succinyl-CoA synthetase in the full TCA cycle.

The found values of attainable maximal cell yield from naphthalene, expressed both by mass ($Y_{X/S}^{max}$) and by energy ($\eta_{X/S}^{max}$), are given together in Table 5. It can be seen that there are two factors affecting the yield: 1) a specific pathway transforming naphthalene to compounds involved in the "usual" metabolism, and 2) features of the tricarboxylic acid cycle. Concerning the pathway of initial naphthalene conversion, the maximal yield estimates belong to two groups. The *meta* path via 2-hydroxymuconate-semialdehyde (2HMS) hydrolase and the *ortho* path give lower yield estimates. At the same time, the *meta* path via 2HMS dehydrogenase and the gentisate pathway give estimates bigger by about 6–7% (0.86/0.81 and 0.8/0.75). All the yields provided by full TCA cycle operation are higher than those provided by the TCA with the glyoxylate bypass by 6.5–9% (Table 5). Hence, the full tricarboxylic acid cycle as well as one of the two naphthalene oxidation paths, the *meta* path via 2HMS dehydrogenase or that via gentisate, if they are present in cells, provide the highest biomass yield from naphthalene, which can be expected as $Y_{X/S}^{max} = 0.86$ by mass, $\eta_{X/S}^{max} = 0.36$ by energy.

It is of interest to compare the above theoretical yield values with experimental ones found during the

Table 4. Forward metabolism (FM) reaction rates, overall input-output FM flow rates and corresponding biomass yield maximal values computed. The case of naphthalene oxidation via the *meta* pathway. Full tricarboxylic acid cycle: variants 1 and 2; glyoxylate bypass: variants 3 and 4. Metabolization of 2-hydroxymuconate semialdehyde via hydrolase: variants 1 and 3; via dehydrogenase: variants 2 and 4.

Reactions	1	2	3	4
	Flows, mmol h^{-1}			
Naphthalene 1,2-dioxygenase	36.2	34.9	38.9	37.2
cis-1,2-Dihydro-1,2-dihydroxynaphthalene dehydrogenase	36.2	34.9	38.9	37.2
1,2-Dihydroxynaphthalene dioxygenase	36.2	34.9	38.9	37.2
2-Hydroxychromene-2-carboxylate isomerase	36.2	34.9	38.9	37.2
trans-o-Hydroxybenzylidenepyruvate hydratase-aldolase	36.2	34.9	38.9	37.2
Salicylaldehyde dehydrogenase	36.2	34.9	38.9	37.2
Salicylate 1-monooxygenase	36.2	34.9	38.9	37.2
Catechol 2,3-dioxygenase	36.2	34.9	38.9	37.2
2-Hydroxymuconate semialdehyde hydrolase	36.2	0	38.9	0
Formate dehydrogenase-N	36.2	0	38.9	0
2-Oxopent-4-enoate hydratase	36.2	34.9	38.9	37.2
4-Hydroxy-2-oxovalerate aldolase	36.2	34.9	38.9	37.2
2-Hydroxymuconate semialdehyde dehydrogenase	0	34.9	0	37.2
γ-Oxalocrotonate isomerase	0	34.9	0	37.2
γ-Oxalocrotonate decarboxylase	0	34.9	0	37.2
Acetaldehyde dehydrogenase	36.2	34.9	38.9	37.2
Pyruvate carboxylase	39.2	38.5	35.5	33.9
Pyruvate dehydrogenase complex	28.4	26.49	37.4	35.8
Phosphoenolpyruvate carboxykinase (ATP)	31.4	30.7	54.9	51.6
Citrate synthase	45.7	42.5	30.2	28.6
Aconitase	45.7	42.5	30.2	28.6
Isocitrate dehydrogenase	45.7	42.5	3	3
Oxoglutarate dehydrogenase	42.7	42.5	0	0
Succinyl coenzyme A synthetase (GTP)	42.7	42.5	0	0
Succinate dehydrogenase (complex II)	42.7	42.5	27.2	25.6
Fumarase (fumarate hydratase)	42.7	42.5	27.2	25.6
Quinone-dependent malate dehydrogenase	43	39.5	55	51.1
Isocitrate lyase	0	0	27.2	25.6
Malate synthase	0	0	27.2	25.6
Enolase	26.6	25.9	50.1	46.8
Phosphoglycerate mutase	26.6	25.9	50.1	46.8
Phosphoglycerate kinase	21.8	21.1	45.3	42
Glyceraldehyde phosphate dehydrogenase (phosphorylating)	21.8	21.1	45.3	42
Triosephosphate isomerase	14.4	13.7	37.9	34.6
Fructose bisphosphate aldolase	14.4	13.7	37.9	34.6
Fructose 1,6-bisphosphatase	14.4	13.7	37.9	34.6
Glucose-6-phosphate isomerase	31.4	29.3	101.9	92
Glucose 6-phosphatase	2	2	2	2
Glucose-6-phosphate dehydrogenase	29.4	27.3	99.9	90
6-Phosphogluconolactonase	29.4	27.3	99.9	90
Phosphogluconate dehydrogenase (decarboxylating)	29.4	27.3	99.9	90
Ribose-5-phosphate isomerase	12.4	11.7	35.9	32.6
D-Ribulose-5-phosphate 3-epimerase	17	15.6	64	57.4
Transketolase (KEGG R01641)	10	9.3	33.5	30.2
Transaldolase (KEGG R08575)	10	9.3	33.5	30.2
Transketolase (KEGG R01067)	7	6.3	30.5	27.2

Table 4. (Contd.)

Reactions	1	2	3	4
	Flows, mmol h^{-1}			
NAD(P)+transhydrogenase (AB-specific)	24	20	165	145
ATP GDP phosphotransferase	42.7	39.5	0	0
ETC (complex I)	155	177	198	216
ETC (complex III)	277	256	319	293
ETC (complex IV)	138	128	160	147
ATP synthase	432	433	518	509
Input-output flows, mmol h^{-1}				
Naphthalene consumed	36.2	34.9	38.9	37.2
O_2 consumed	283	268	315	295
CO_2 formed	211	198	237	221
H_2O formed	400	395	411	404
$\eta_{X/S}^{max}$	0.35	0.36	0.33	0.34
$Y_{X/S}^{max}$, g/g	0.82	0.86	0.77	0.8

Table 5. Values of maximal biomass yield from naphthalene when it is oxidized via different pathways. Abbreviations: TCA, tricarboxylic acid cycle; 2HMS, 2-hydroxymuconate semialdehyde.

Pathway of naphthalene oxidation		Full TCA		Glyoxylate bypass		$\frac{yield_{full\ TCA}^{max}}{yield_{glyoxylate\ bypass}^{max}}$
		$Y_{X/S}^{max}$	$\eta_{X/S}^{max}$	$Y_{X/S}^{max}$	$\eta_{X/S}^{max}$	
Ortho		0.81	0.34	0.75	0.32	1.080
Via gentisate		0.86	0.36	0.79	0.33	1.089
Meta	via 2HMS hydrolase	0.82	0.35	0.77	0.33	1.065
	via 2HMS dehydrogenase	0.86	0.36	0.8	0.34	1.075
	$\frac{yield_{2HMS\ hydrolase}^{max}}{yield_{2HMS\ dehydrogenase}^{max}}$	1.05		1.04		

cultivation of various organisms on naphthalene and other substrates.

There are few experimental yield values for naphthalene present in literature. Volkering et al. [8] published $Y_{X/S} = 1.2$, which is considerably higher than the theoretical values found here. The likelihood of this value can be considered in comparison with microbial growth on *n*-alkanes. This process was widely investigated in connection with its industrial applications [31–34]. The reliable value of the maximal yield from *n*-alkanes in the absence of additional substrates such as the yeast extract was found to be 1.0–1.1 g/g. The mass yield value from naphthalene, $\eta_{X/S}$, with the same energetic yield $\eta_{X/S}$ as that from *n*-alkanes, according to Eq. (10) in **MATERIALS AND METHODS**, equals $1.1 \times 0.875 = 0.96$. It should be taken into account that metabolization of *n*-alkanes includes one O_2-consuming stage not coupled with ATP formation, viz., a monooxygenase. At the same time, metabolization of naphthalene includes several oxygenase reactions and, therefore, results in a larger energy loss. For this reason, the yield from naphthalene should be lower – but in no way higher – than 0.96, which is consistent with the yield values found in the present work. Thus, the mentioned experimental value $Y_{X/S} = 1.2$ is overstated, which can be because of problems with the accuracy of the consumed substrate measurement.

Another data set obtained during cultivation of *Bacillus thermoleovorans* on naphthalene [9] presents values of cell biomass yield by carbon, $y_{X/S}$, which is the ratio of carbon of cells grown to carbon of the substrate consumed. The maximal value of $y_{X/S}$ found in that work is 0.21. According to Eq. (11) (**MATERIALS AND METHODS**), the mass yield from naphthalene is

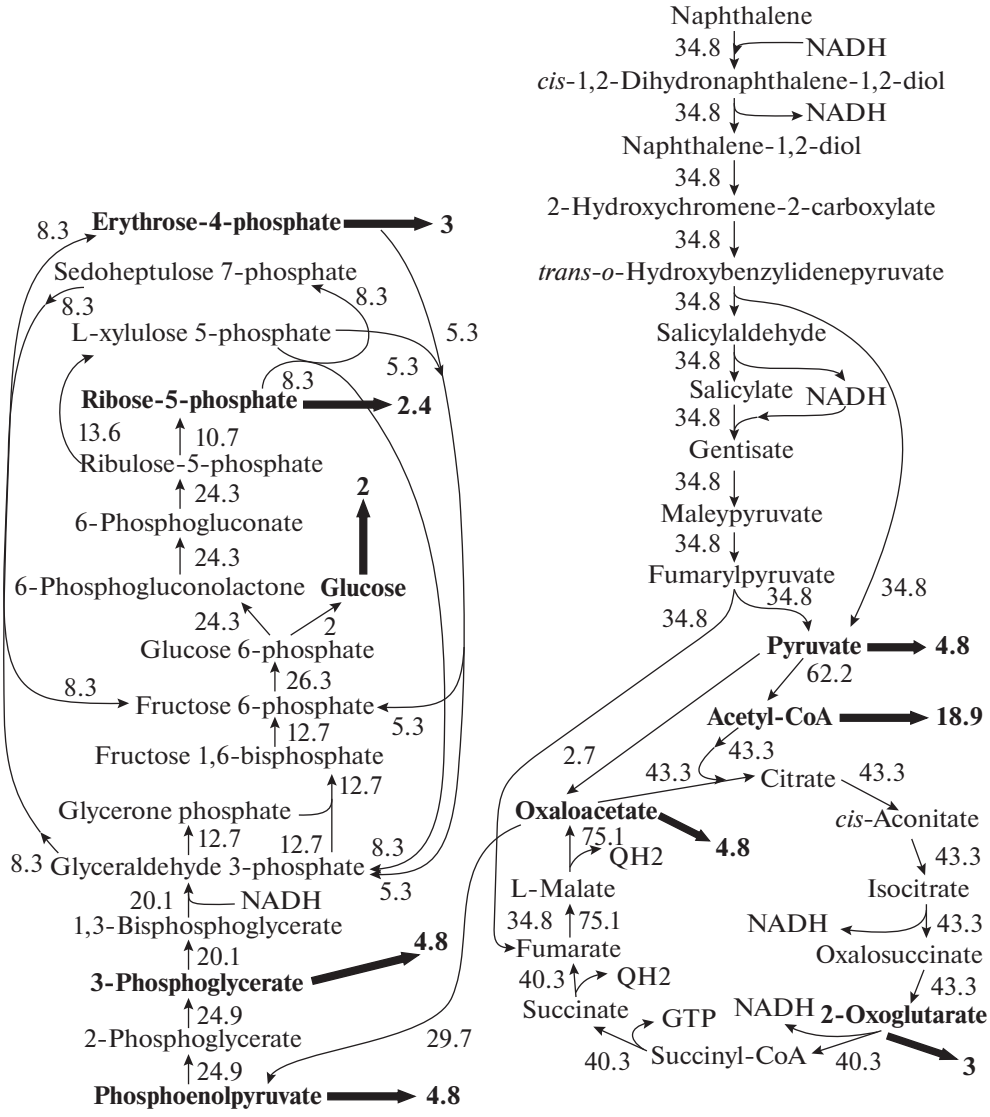

Fig. 2. Scheme of nodal metabolite (NM) synthesis from naphthalene via the pathway via gentisate (variant 1 in Table 3 for $Y^{max}_{X/Naphthalene} = 0.86$). NM names are given by Arial bold. Thick arrows show outflows of NM formed in the forward metabolism to the standard constructive metabolism (see Table 1).

$Y_{X/S} = 0.43$. This value is markedly lower than the maximal upper limit found in the present work.

Comparison of the found theoretical yield maximum from naphthalene with the biomass yield from other substrates can be correctly done using energetic growth efficiency $\eta_{X/S}$ which is independent of substrate energy content in its mass unit. As mentioned above, a reliable maximal value of $\eta_{X/S}$ was achieved during the growth of various microorganisms on glucose, viz., 0.6. The estimates of maximal energy yield values from naphthalene obtained in the present work are markedly lower: about 1/3 (Table 5). Nearly half of naphthalene energy, which could be utilized by cells if the efficiency of its utilization had been the same as on glucose, is actually lost. The reason is the occurrence of several oxygenase reactions which oxidize naphthalene and its intermediates without coupling with ATP formation. Further, $Y_{X/S} = 1.1$ for growth on *n*-alkanes, according to Eq. (6), gives $\eta_{X/S} = 0.41$. Methanol-assimilating microorganisms show $\eta_{X/S} = 0.32–0.36$ (yeasts) and $\eta_{X/S} = 0.41–0.46$ (bacteria) [20]. Energetic efficiency of methanol-grown yeasts is close to the estimates of this quantity for naphthalene degrading bacteria found in the present work. This fact is due to a similar part of energy losses on naphthalene and on methanol: yeasts oxidize methanol to formaldehyde without ATP formation. In

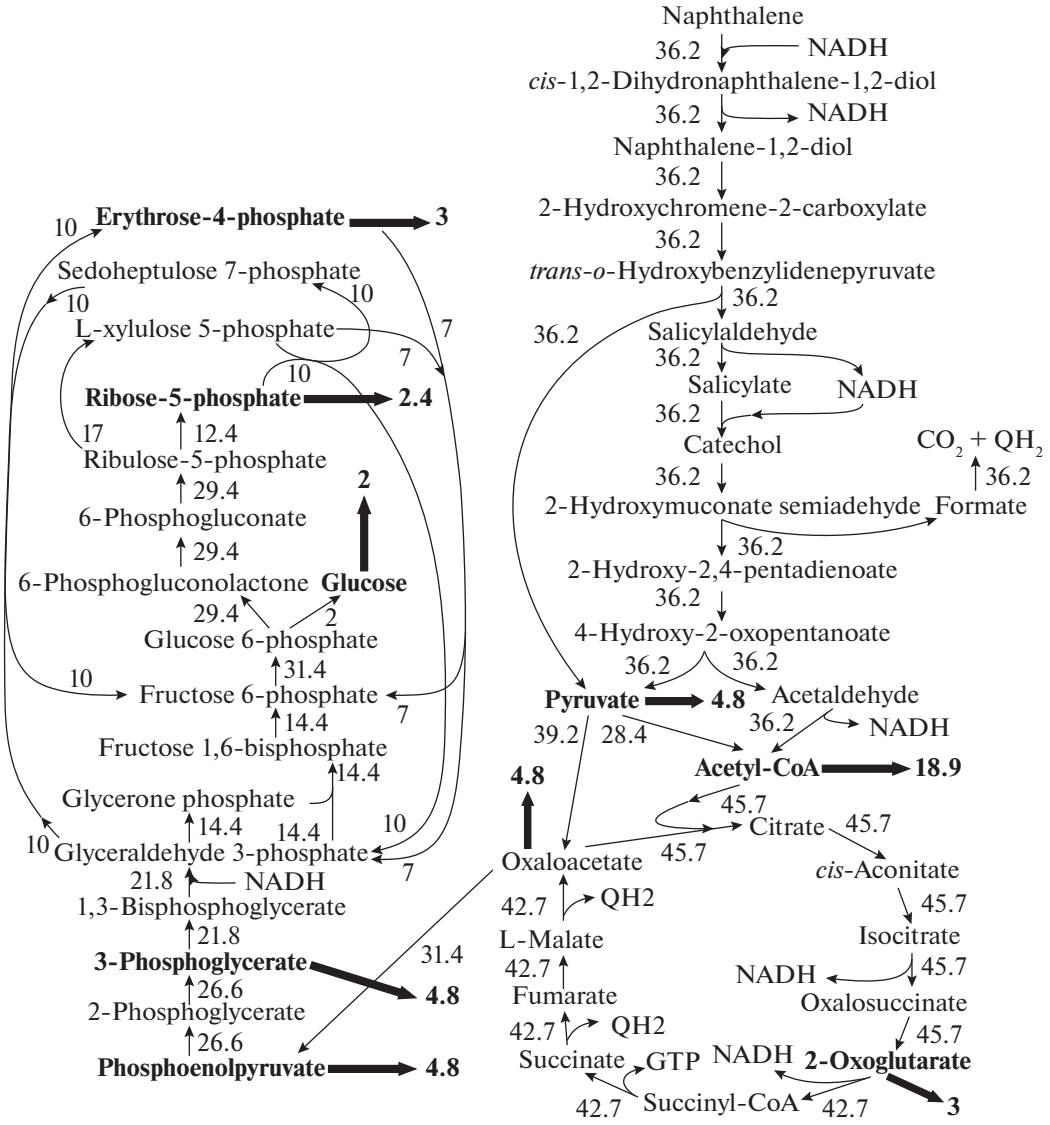

Fig. 3. Scheme of nodal metabolite (NM) synthesis from naphthalene via the *meta* pathway (variant 1 in Table 4 for $Y^{max}_{X/Naphthalene} = 0.82$). NM names are given by Arial bold. Thick arrows show outflows of NM formed in the forward metabolism to the standard constructive metabolism (see Table 1).

methanol-assimilating bacteria there is partial coupling of methanol oxidation to formaldehyde with ATP formation due to which bacterial $\eta_{X/S}$ on methanol is higher than that of yeasts on methanol and bacteria on naphthalene. Comparison of $\eta_{X/S}$ given here shows that conversion of naphthalene to cell biomass has one of the lowest energetic efficiency values.

CONCLUSION

Our study, using mathematical and computer biochemistry tools, elucidates the patterns of reaction rates composing the forward part of metabolism in cells degrading naphthalene. For every pathway of naphthalene oxidation we found the maximal biomass yield value which cannot be exceeded during the growth of bacteria on this substrate in a fermentor or in soil. The results obtained show that the maximum biomass yield from naphthalene depends notably on the peculiarities of that part of cell metabolism, which is not specific for this particular substrate. Comparison of interrelations between various reaction rates within the forward metabolism, found in our work, with similar interrelations present in a strain of interest can help to find a bottleneck step which determines the maximal rate of naphthalene degradation by this organism. Revealing such a bottleneck, in turn, may serve as an indication on genes the amplification of which could increase the degradation rate.

APPENDIX

Table A1. Reactions present in the local database which was used for construction of the forward metabolism in naphthalene degrading bacteria. The reactions are designated by names of the corresponding enzymes. Left aligned bold numbers indicate irreversible reactions

No.	Reaction	No.	Reaction
1	ETC (complex I)	40	Glyoxylate reductase
2	ETC (complex III)	**41**	Glucose 6-phosphatase
3	ETC (complex IV)	**42**	Fructose 1,6-bisphosphatase
4	ATP synthase	43	Maleylpyruvate isomerase
5	Catalase	44	Glucose-6-phosphate dehydrogenase
6	$NAD(P)^+$ transhydrogenase (AB-specific)	45	6-Phosphogluconolactonase
7	ATP-GDP phosphotransferase	**46**	Phosphogluconate dehydrogenase (decarboxylating)
8	Hexokinase	47	Ribose-5-phosphate isomerase
9	Glucose-6-phosphate isomerase	48	D-ribulose-5-phosphate 3-epimerase
10	6-Phosphofructokinase	49	Transketolase (KEGG R01641)
11	Fructose bisphosphate aldolase	50	Transaldolase (KEGG R08575)
12	Triosephosphate isomerase	51	Transketolase (KEGG R01067)
13	Glyceraldehyde phosphate dehydrogenase (phosphorylating)	52	3-Hexulose-6-phosphate synthase
14	Phosphoglycerate kinase	53	6-Phospho-3-hexuloisomerase
15	Phosphoglycerate mutase	**54**	Glycerol kinase
16	Enolase	55	Glycerol-3-phosphate 1-dehydrogenase (NADP+)
17	Pyruvate kinase	56	Glycerol NAD^+ oxidoreductase
18	Pyruvate decarboxylase	**57**	Triose kinase
19	Alcohol dehydrogenase	58	Aldehyde dehydrogenase (NAD+)
20	Pyruvate dehydrogenase complex	**59**	Glycerate 3-kinase
21	Pyruvate carboxylase	**60**	Glycerate-2-kinase
22	Phosphoenolpyruvate carboxykinase (ATP)	61	Glycerol NAD+ 2-oxidoreductase
23	Phosphoenolpyruvate carboxylase	62	Glycerol-3-phosphate dehydrogenase (NAD^+)
24	Citrate synthase	63	Glycerol-3-phosphate dehydrogenase [$NAD(P)^+$]
25	Aconitase (step 1)	**64**	Glycerone kinase
26	Aconitase (step 2)	**65**	Phosphoenolpyruvate-glycerone phosphotransferase
27	Isocitrate dehydrogenase (step 1)	66	3-Fumarylpyruvate hydrolase
28	Isocitrate dehydrogenase (step 2)	**67**	Methane monooxygenase
29	Oxoglutarate dehydrogenase	**68**	Methanol cytochrome cL oxidoreductase
30	Succinyl coenzyme A synthetase (GTP)	**69**	Alcohol oxidase
31	Succinate dehydrogenase (complex II)	**70**	Formaldehyde dehydrogenase
32	Fumarase (fumarate hydratase)	**71**	Formate dehydrogenase-N
33	Malate dehydrogenase (NAD-dependent)	72	Formaldehyde transketolase
34	Quinone-dependent malate dehydrogenase	73	Serine transhydroxymethylase
35	Acetyl Co-A synthetase	74	Serine-glyoxylate transaminase
36	Lactate dehydrogenase	75	Glycerate dehydrogenase
37	Acetaldehyde dehydrogenase	76	Malyl-CoA lyase (acetyl-CoA forming)
38	Isocitrate lyase	**77**	CoA-independent aldehyde dehydrogenase (NAD)
39	Malate synthase	78	Succinyl-CoA-malate CoA transferase

No.	Reaction	No.	Reaction
79	Malate-CoA ligase	**98**	3-Oxoadipate enol-lactonase
80	Tetrahydroxynaphthalene reductase	99	Acetylsalicylate deacetylase
81	Salicylaldehyde dehydrogenase	100	Acylpyruvate hydrolase
82	1,6-Dihydroxycyclohexa-2,4-diene-1-carboxylate dehydrogenase	101	2-Hydroxymuconate-semialdehyde hydrolase
83	*cis*-1,2-Dihydro-1,2-dihydroxynaphthalene dehydrogenase	**102**	4-Carboxymuconolactone decarboxylase
84	Dibenzothiophene dihydrodiol dehydrogenase	**103**	6-Methylsalicylate decarboxylase
85	Catechol 1,2-dioxygenase	**104**	Salicylate decarboxylase
86	Catechol 2,3-dioxygenase	105	*trans-o*-Hydroxybenzylidenepyruvate hydratase-aldolase
87	Protocatechuate 3,4-dioxygenase	106	4-Hydroxy-2-oxovalerate aldolase
88	Gentisate 1,2-dioxygenase	107	2-Oxopent-4-enoate hydratase
89	1,2-Dihydroxynaphthalene dioxygenase	108	Muconolactone delta-isomerase
90	Benzoate 1,2-dioxygenase	109	Muconate cycloisomerase
91	Naphthalene 1,2-dioxygenase	110	3-Carboxy-*cis*,*cis*-muconate cycloisomerase
92	Salicylate 1-monooxygenase	111	2-Hydroxychromene-2-carboxylate isomerase
93	4-Hydroxybenzoate 3-monooxygenase	112	2-Hydroxymuconate semialdehyde dehydrogenase
94	Benzoate 4-monooxygenase	113	γ-Oxalocrotonate isomerase
95	Salicylate 5-hydroxylase	**114**	γ-Oxalocrotonate decarboxylase
96	3-Oxoadipyl-CoA thiolase	**115**	Gentisate 1,2-dioxygenase
97	3-Oxoadipate CoA-transferase		

Table A2. Substrates and products of the reactions present in the local database which was used for construction of the forward metabolism in naphthalene degrading bacteria

No.	Compounds	No.	Compounds
1	O_2	18	$NADP^+$
2	CO_2	19	Ubiquinol (QH_2)
3	H_2O	20	Ubiquinone (Q)
4	H_2O_2	21	Ferrocytochrome C^{2+}
5	$H^{(+in)}$	22	Ferricytochrome C^{3+}
6	$H^{(+out)}$	23	CoA
7	H_3PO_4	24	Acetyl-CoA
8	Pyrophosphate	25	Succinyl-CoA
9	ATP	26	3-Oxoadipyl-CoA
10	ADP	27	L-Malyl-CoA
11	AMP	28	Tetrahydrofolate
12	GTP	29	5,10-Methylenetetrahydrofolate
13	GDP	30	D-Glucose
14	GMP	31	D-Glucose 6-phosphate
15	NADH	32	D-Fructose 6-phosphate
16	NAD^+	33	D-Fructose 1,6-bisphosphate
17	NADPH	34	Glycerone phosphate

No.	Compounds	No.	Compounds
35	D-Glyceraldehyde 3-phosphate	74	Formaldehyde
36	1,3-Bisphosphoglycerate	75	Formate
37	3-Phosphoglycerate	76	1,6-Dihydroxycyclohexa-2,4-diene-1-carboxylate
38	2-Phosphoglycerate	77	5-Oxo-2,5-dihydrofuran-2-acetate
39	Phosphoenolpyruvate	78	1,2-Dihydroxydibenzothiophene
40	Pyruvate	79	1,3,6,8-Naphthalenetetrol
41	Acetaldehyde	80	2,5-Dihydro-5-oxofuran-2-acetate (Muconolactone)
42	Ethanol	81	2,5-Dihydroxybenzoate (Gentisate)
43	Acetate	82	2-Carboxy-2,5-dihydro-5-oxofuran-2-acetate
44	Lactate	83	2-Hydroxy-2,4-pentadienoate
45	3-Hydroxypyruvate	84	2-Hydroxychromene-2-carboxylate
46	Citrate	85	2-Hydroxymuconate semialdehyde
47	*cis*-Aconitate	86	2-Oxo-2,3-dihydrofuran-5-acetate (3-Oxoadipate enol-lactone)
48	Isocitrate	87	3,4-Dihydroxybenzoate
49	Oxalosuccinate	88	3-Carboxy-cis,cis-muconate
50	2-Oxoglutarate	89	3-Cresol
51	Succinate	90	3-Fumarylpyruvate
52	Fumarate	91	3-Oxoadipate
53	L-Malate	92	4-Hydroxy-2-oxopentanoate
54	Oxaloacetate	93	4-Hydroxybenzoate
55	Glyoxylate	94	6-Methylsalicylate
56	Glycolate	95	Aspirin (Acetylsalicylate)
57	6-Phosphogluconolactone	96	Benzoate
58	6-Phosphogluconate	97	Catechol
59	D-Ribulose 5-phosphate	98	*cis*-1,2-Dihydronaphthalene-1,2-diol
60	D-Ribose 5-phosphate	99	*cis*-1,2-Dihydroxy-1,2-dihydrodibenzothiophene
61	D-Xylulose 5-phosphate	100	*cis,cis*-Muconate
62	Sedoheptulose 7-phosphate	101	Gentisate aldehyde
63	D-Erythrose 4-phosphate	102	Homogentisate
64	D-Arabino-hex-3-ulose 6-phosphate	103	Maleylpyruvate
65	Glycerol	104	Naphthalene-1,2-diol
66	*sn*-Glycerol 3-phosphate	105	Naphthalene
67	D-Glyceraldehyde	106	Phenol
68	D-Glycerate	107	Salicylaldehyde
69	Glycerone	108	Salicylate
70	Glycine	109	Scytalone
71	L-Serine	110	*trans-o*-Hydroxybenzylidenepyruvate
72	Methane	111	2-Hydroxymuconate
73	Methanol	112	γ-Oxalocrotonate

REFERENCES

1. *Cerniglia C.E.* Biodegradation of polycyclic aromatic hydrocarbons. *Biodegr.*, 1992, 3(2-3), 351–368. https://doi.org/10.1007/BF00129093
2. *Zylstra G.J., Kim E., Gloyal A.K.* Comparative molecular analysis of genes for polycyclic aromatic hydrocarbon degradation. *Gen. Eng.,* 1997, 19, 257–269.
3. *Tomás-Gallardo L., Gómez-Álvarez H., Santero E., Floriano B.* Combination of degradation pathways for naphthalene utilization in *Rhodococcus* sp. strain TFB. *Microbial Biotechnol.*, 2014, 7(2), 100–113. Epub 2013 Dec 11. https://doi.org/10.1111/1751-7915.12096
4. *Ghosal D., Ghosh S., Dutta T.K., Ahn Y.* Current state of knowledge in microbial degradation of polycyclic aromatic hydrocarbons (pahs): A review. *Front. Microbiol.*, 2016, 7:1369 https://doi.org/10.3389/fmicb.2016.01369
5. *Nogales J., Garcia J.L., Diaz E.* Degradation of Aromatic Compounds in *Pseudomonas*: A Systems Biology View. In: Aerobic Utilization of Hydrocarbons, Oils and Lipids. Handbook of Hydrocarbon and Lipid Microbiology, Rojo, F., ed. (Springer, Cham). 2017, pp. 1–49. https://doi.org/10.1007/978-3-319-39782-5_32-1.
6. *Dutta K., Shityakov S., Khaifa I., Ballav S., Jana D., Manna T., Karmakar M., Raul P., Guchhait K.C., Ghosh C.* Enhanced biodegradation of naphthalene by *Pseudomonas* sp. consortium immobilized in calcium alginate beads. BioRxiv, 2019. https://doi.org/10.1101/631135
7. *Mohapatra B., Phale P.S.* Microbial degradation of naphthalene and substituted naphthalenes: metabolic diversity and genomic insight for bioremediation. *Front. Bioeng. Biotechnol.*, 2021, https://www.frontiersin.org https://doi.org/10.3389/fbioe.2021.602445.
8. *Volkering F., Breure A.M., van Andel J.G.* Effect of microorganisms on the bioavailability and biodegradation of crystalline naphthalene. *Appl. Microbiol. Biotechnol.*, 1993, 40(4), 535–540.
9. *Annweiler E., Richnow H.H., Antranikian G., Hebenbrock S., Garms C., Franke S., Francke W., Michaelis W.* Naphthalene degradation and incorporation of naphthalene derived carbon into biomass by the thermophile *Bacillus thermoleovorans*. *Appl. Environ. Microbiol.*, 2000, 66(2), 518–523. https://doi.org/10.1128/aem.66.2.518-523.2000
10. *Minkevich I.G.* Estimation of maximal values of biomass growth yield based on the mass-energy balance of cell metabolism. *Comp. Res. Model.*, 2019, 11(4), 723–750. http://crm.ics.org.ru/uploads/crmissues/crm_2019_4/-2019_04_11.pdf https://doi.org/10.20537/2076-7633-2019-11-4-723-750
11. *Minkevich I.G.* The effect of cell metabolism on biomass yield during the growth on various substrates. *Comp. Res. Model.*, 2017, 9(6). 993–1014. http://crm.ics.org.ru/uploads/crmissues/crm_2017_6/2017_06_11.pdf https://doi.org/10.20537/2076-7633-2017-9-6-993-1014
12. *Minkevich I.G.* Stoichiometric synthesis of metabolic pathways. *Comp. Res. Model.*, 2015, 7(6), 1241–1267. http://crm.ics.org.ru/uploads/crmissues/crm_2015_-6/15.07.07.pdf
13. *Minkevich I.G.* Mathematical problems of metabolic pathway organization from biochemical reactions. *Math. Biol. Bioinform*. 2016, 11(2), 406–425. https://doi.org/10.17537/2016.11.406
14. *Pirt S.J.* Principles of Microbe and Cell Cultivation. 1975, London, Edinburgh, Melbourne, Blackwell Sci. Publ., Oxford. Corpus ID: 85672088.
15. *Minkevich I.G.* Mass-energy Balance and Kinetics of the Growth of Microorganisms. 2005, Moscow–Izhevsk, Regular and Chaotic Dynamics.
16. *Minkevich I.G., Eroshin V.K.* Productivity and Heat Generation of Fermentation Under Oxygen Limitation. *Folia Microbiol.*, 1973, 18(5), 376–385. https://doi.org/10.1007/BF02875932
17. *Erickson L.E., Minkevich I.G., Eroshin V.K.* Application of mass and energy balance regularities in fermentation. *Biotechnol. Bioeng.*, 1978, 20(10), 1595–1621.
18. *Erickson L.E., Minkevich I.G., Eroshin V.K.* Utilization of Mass-Energy Balance Regularities in the Analysis of Continuous Culture Data. *Biotechnol. Bioeng.*, 1979, 21(4), 575–591.
19. *Minkevich I.G.* Physico-chemical properties of organic compounds and the energetics of metabolism. *J. Theor. Biol.*, 1982, 95(3), 569–590. https://doi.org/10.1016/0022-5193(82)90035-2
20. *Minkevich I.G.* Estimation of available efficiency of microbial growth on methanol and ethanol. *Biotechnol. Bioeng.*, 1985, 27(6), 792–799. https://doi.org/10.1002/BIT.260270607 Corpus ID: 44297873
21. *Aris R.* Prolegomena to the rational analysis of systems of chemical reactions. *Arch. Rational Mech. Anal.*, 1965, 19, 81–99.
22. *Mogi T., Murase Y., Mori M., Shiomi K., Omura S., Paranagama M.P., Kita K.* Polymyxin B identified as an inhibitor of alternative NADH dehydrogenase and malate:quinone oxidoreductase from the Gram-positive bacterium *Mycobacterium smegmatis*. *J. Biochem.*, 2009, 146(4), 491–499. https://doi.org/10.1093/jb/mvp096
23. *Mellgren E.M., Kloek A.P., Kunkel B.N.* MQO, a tricarboxylic acid cycle enzyme, is required for virulence of *Pseudomonas syringae* pv. tomato strain DC3000 on *Arabidopsis thaliana*. *J. Bacteriol.,* 2009, 191(9), 3132-3141. https://doi.org/10.1128/JB.01570–08
24. *Igeno M.I., Becerra G., Guijo M.I., Merchan F., Blasco R.* Metabolic adaptation of *Pseudomonas pseudoalcaligenes* CECT5344 to cyanide: role of malate-quinone oxidoreductases, aconitase and fumarase isoenzymes. *Biochem. Soc. Trans.*, 2011, 39(6), 1849–1853. https://doi.org/10.1042/BST20110714
25. *Luque-Almagro V.M., Merchan F., Blasco R., Igeno M.I., Martinez-Luque M., Moreno-Vivian C., Castillo F., Roldan M.D.* Cyanide degradation by *Pseudomonas pseudoalcaligenes* CECT5344 involves a malate:quinone oxidoreductase and an associated cyanide-insensitive electron transfer chain. *Microbiol.*, 2011, 157, 739–746. https://doi.org/10.1099/mic.0.045286-0
26. *Kabashima Y., Sone N., Kusumoto T., Sakamoto J.* Purification and characterization of malate:quinone ox-

idoreductase from thermophilic *Bacillus* sp. PS3. *J. Bioenerg. Biomembr.*, 2013, 45, 131–136. https://doi.org/10.1007/s10863-012-9485-5

27. *Takahashi-Iniguez T., Aburto-Rodriguez N., Vilchis-Gonzalez A.L., Flores M.E.* Function, kinetic properties, crystallization, and regulation of microbial malate dehydrogenase. *J. Zhejiang Univ-Sci. B (Biomed. Biotechnol.)*, 2016, 17(4), 247–261. https://doi.org/10.1631/jzus.B1500219.
28. *Payne W.J.* Energy yields and growth of heterotrophs. *Ann. Rev. Microbiol.*, 1970, 24, 17–52. https://doi.org/10.1146/annurev.mi.24.100170.000313
29. *Minkevich I.G., Dedyukhina E.G., Chistyakova T.I.* The effect of lipid content on the elemental composition and energy capacity of yeast biomass. *Appl. Microbiol. Biotechnol.*, 2010, 88(3), 799–806. https://doi.org/10.1007/s00253-010-2766-1 Corpus ID: 32925563
30. *Minkevich I.G., Fursova P.V., Tjorlova L.D., Tsygankov A.A., Riznichenko G.Yu.* The stoichiometry and energetics of oxygenic phototrophic growth. *Photosyn. Res.*, 2013, 116(1), 55–78. https://doi.org/10.1007/s11120-013-9896-0
31. *Ertola R.J., Mazza L.A., Balatti A.P.* Composition of cell material and biological value of the cellular protein of a *Micrococcus* strain grown on hydrocarbons. *Biotechnol. Bioeng.*, 1969, 11(3), 409–416. https://doi.org/10.1002/bit.260110312
32. *Wagner F., Kleemann T., Zahn W.* Microbial transformation of hydrocarbons. II. Growth constants and cell composition of microbial cells derived from n-alkanes. *Biotechnol. Bioeng.*, 1969, 11(3), 393–408. https://doi.org/10.1002/bit.260110311
33. *Johnson M.J.* Microbial Cell Yields from Various Hydrocarbons. In: Fermentation Advances. *Perlman D* (ed.) New York, London, Academic Press, 1969, pp 833–842.
34. *Sukatsch D., Johnson M.J.* Bacterial cell production from hexadecane at high temperatures. *Biotechnol. Bio eng.,* 1972, 23, 543–546. https://doi.org/10.1128/AEM.23.3.543-546.1972 Corpus ID: 34303650

Максимальный выход биомассы из нафталина: теоретическая оценка, основанная на свойствах метаболизма клеток

И. Г. Минкевич[a, #], И. А. Кошелева[a], А. М. Боронин[a]

[a]Институт биохимии и физиологии микроорганизмов им. Г.К. Скрябина, ФИЦ Пущинский научный центр биологических исследований РАН, Пущино, Московская обл., 142290 Россия

[#]e-mail: minkevich@ibpm.pushchino.ru

Метаболические пути конверсии нафталина в набор соединений-предшественников образования биомассы и полные совокупности скоростей соответствующих биохимических реакций найдены с помощью компьютерной реконструкции. Использованы стехиометрические коэффициенты реакций и данные об их обратимости или необратимости. Найденные скорости синтеза предшественников образования биомассы и использование биоэнергетических закономерностей метаболизма дали значения максимального выхода биомассы. Найдено, что наличие в клетках таких путей окисления нафталина, как *мета*, *орто* или путь через гентизат, оказывает меньшее влияние на величину выхода биомассы, чем функционирование цикла трикарбоновых кислот через полную последовательность или через глиоксилатный шунт. Последний фактор заметно влияет на величины потоков через глюконеогенез и пентозофосфатный путь. Найдено, что максимальный выход биомассы из нафталина находится в пределах 0.75–0.86 г/г. Максимальная доля энергетического содержания нафталина, переходящая в образованную биомассу — примерно 1/3.

Ключевые слова: разложение нафталина, бактерии, метаболизм клеток, стехиометрия совокупностей реакций, выход биомассы, биоэнергетика